Theoretical Study of Singlet and Triplet Excitation Energies in Oligothiophenes

E. Fabiano,* F. Della Sala, and R. Cingolani

National Nanotechnology Laboratory of INFM, Distretto Tecnologico, Università degli Studi di Lecce, Via per Arnesano, I-73100 Lecce, Italy

M. Weimer and A. Görling

Lehrstuhl für Theoretische Chemie, Universität Erlangen-Nürnberg, Egerlandstr. 3, 91058 Erlangen, Germany

Received: November 3, 2004; In Final Form: February 4, 2005

We have analyzed singlet and triplet excitation energies in oligothiophenes (up to five rings) using time-dependent density-functional theory (TD-DFT) with different exchange-correlation functionals and compared them with results from the approximate coupled-cluster singles and doubles model (CC2) and experimental data. The excitation energies have been calculated in geometries obtained by TD-DFT optimization of the lowest excited singlet state and in the ground-state geometries of the neutral and anionic systems. TD-DFT methods underestimate photoluminescence energies but the energy difference between singlet and triplet states shows trends with the chain-length similar to CC2. We find that the second triplet excited state is below the first singlet excited state for long oligomers in contrast with the previous assignment of Rentsch et al. (*Phys. Chem. Chem. Phys.* **1999**, *1*, 1707). Their photodetachment photoelectron spectroscopy measurements are better described by considering higher triplet excited states.

I. Introduction

In recent years, conjugated organic oligomers and polymers have raised an increasing interest due to their peculiar electronic and optical properties and to their application as new materials for electronic[1] and optoelectronic devices.[2] Among such oligomers,[3] oligothiophenes represent a very important example: their optical properties have been the subject of numerous investigations both experimental and theoretical.[4] In particular the knowledge about the relative energetic position of singlet and triplet excited-states is of fundamental importance to understand the photophysics of oligothiophenes.[5−9]

To manage the complexity of these systems, the optical properties of oligothiophenes have been calculated for a long time by semiempirical methods.[5,10−15] These methods can be easily applied to large systems but an exact quantitative estimate of electronic properties is difficult due to the use of empirical parameters and an insufficient/incorrect description of the electron−electron interaction effects. Thus, a first-principles investigation is needed to obtain a deeper quantitative insight into the properties of these systems. So far, correlated ab initio calculations of excited states of oligothiophenes have only appeared for the monomer[16−18] and for bithiophene,[9,19] due to the required high computational cost.

Time-dependent density functional theory (TD-DFT)[20−25] has attracted a lot of interest because it includes electronic correlation in an efficient manner, thus allowing the investigation of large systems. However, the capability of TD-DFT to predict correctly the chain length evolution is under debate.[26−36] Various studies on oligothiophenes using TD-DFT have already appeared.[37−39] In these works, the evolution of the lowest singlet/triplet excitation energies with the number of monomers is reported. Although it is known that higher singlet states lie very high in energy,[4,5,8] higher triplet states and their energies have not been carefully investigated so far. Moreover, the dependence of the previously obtained results on the choice of the approximate exchange-correlation (XC) functionals needs further investigation.

Furthermore, theoretical investigations of the optical properties of oligothiophenes have been performed mainly by studying absorption spectra,[5,8,10−15,37−39] i.e., by carrying out calculations of excitation energies of the systems in their ground-state geometries, because efficient and accurate tools for the computation of excited-state geometries and the subsequent calculation of emission energies were not available so far. Using the CIS (configuration interaction singles) method[40] for geometries and TD-DFT for excitation energies might cause inconsistent results in the evaluation of the Stokes shifts.[32−34] By a recently developed TD-DFT gradient method,[41] it is now possible to optimize the geometry of individual singlet or triplet excited-states. This method has the same computational cost but is much more accurate than the CIS method, and it has been successfully applied to the calculation of emission energies of thiophene derivatives.[42,43]

In this work, we investigate the accuracy of TD-DFT to predict emission energies and triplet excitation energies in oligothiophenes. The influence of different approximations for the XC functional is studied by employing a wide variety of functionals of increasing quality. Calculated energies are compared with fluorescence[44] and photodetachment photoelectron spectroscopy (PD-PES)[7] measurements and are used for the reassignment of the experimental peaks.

Moreover the TD-DFT approaches are compared with the approximate coupled-cluster singles and doubles model (CC2),[45] a size-consistent correlated ab initio method, which is known to be reliable for the description of the chain-length dependence of excitation energies of organic chainlike molecules.[28,46]

* To whom correspondence should be addressed.

10.1021/jp044974f CCC: $30.25
Published on Web 03/12/2005

II. Methods

We report the TD-DFT lowest singlet and triplet excitation energies for oligothiophenes with 2, 3, 4, and 5 rings (hereafter *nT* where *n* is the number of rings).

The monomer is not investigated here because it behaves qualitatively differently from its oligomers. This peculiar behavior of the thiophene monomer, compared to its oligomers, can be related to the presence of many low-lying Rydberg orbitals in the orbital spectrum.[18] Because of the different symmetry of the oligomers, C_{2v} for 3*T* and 5*T* and C_{2h} for 2*T* and 4*T*, the states investigated are either $^1B_1$ and $^3B_1$, $^3A_1$ or ^1B_u and ^3B_u, ^3A_g. For simplicity, without ambiguity, we choose to refer to them just as ^1B and ^3B, ^3A states.

Several XC functionals have been used to carry out TD-DFT calculations, to understand the influence of the different degrees of approximations on the calculated excitation energies. If it is not stated differently, a considered XC potential used in the KS ground-state calculation is accompanied by the corresponding adiabatic, i.e., frequency independent, XC kernel in the TD-DFT calculations.

As a first choice, we have used the local density approximation (LDA), which already has been employed to compute excitation energies of oligothiophenes in the past.[8,37]

The natural improvement of the LDA description is the generalized gradient approximation (GGA)[47] that is expected to treat better small charge density inhomogeneities. In our calculations, we have used the Becke-Perdew (B−P) functional.[48,49] However it is well-known that for excitation energies GGA functionals yield similar results as LDA functionals.[25]

The use of hybrid functionals can highly improve the accuracy by including exact Hartree−Fock exchange.[25] To this end we have used the B3-LYP functional.[50]

A major problem of LDA, GGA, and even hybrid functionals is the presence of unphysical Coulomb self-interactions.[51−53] As a result, only a few Kohn−Sham (KS) virtual orbitals are bound, and this can influence the quality of TD-DFT results which are based on the whole KS eigenvalue spectrum. One possible solution is to use the localized Hartree−Fock (LHF) potential, a local effective exact-exchange KS potential, to obtain self-interaction free KS orbitals.[54,55] We combine the LHF approach for the KS ground-state calculation with a TD-DFT calculation which employs the Becke exchange kernel.[48]

Finally, results from the approximate coupled-cluster singles and doubles model (CC2) with the resolution of identity approximation[56] have been computed in order to compare DFT results with size-consistent correlated ab initio results.

All these methods have been applied to geometries obtained by TD-DFT B3-LYP optimization of the lowest singlet excited-state, the ^1B state. Thus, the calculated ^1B state excitation energies represent the photoluminescence energies. The ^1B state geometry is planar, according to TD-DFT optimization and analysis of absorption-luminescence spectra.[44]

We also consider two other planar geometries, those of neutral ground-states and of the anions. In this way, we can study the evolution of the lower excited states when going from aromatic to quinoid character, without considering torsional effects. In particular, the anion ground-state geometry (which is almost planar) has been chosen to obtain theoretical results comparable to experimental data from PD-PES.[7] In fact in PD-PES, an electron is detached by a laser pulse from a charged molecule leaving it either in a singlet or a triplet state, without selection rules, and the energy of the resulting molecular state is determined by measuring the energy of the detached electron.[59]

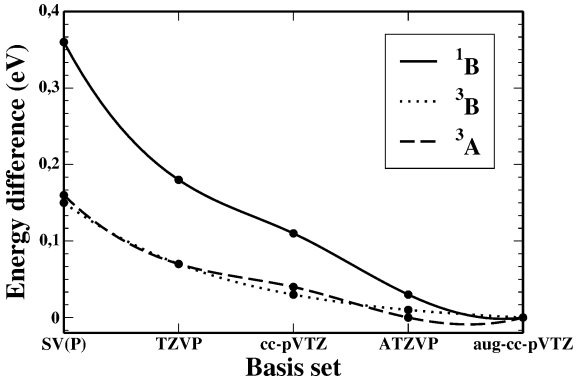

Figure 1. Difference between excitation energies of the first singlet and of the two lowest triplet states of 3*T* computed at the CC2 level with the indicated basis set and the respective excitation energy computed with aug-cc-pVTZ basis set.

Note that in the comparison of the different methods employed to calculate the excitation energies we always use the same geometries, i.e., those obtained by optimization with the B3-LYP functional.

III. Computational Details

Geometry optimizations have been performed using DFT for ground-state geometries and TD-DFT[41] for excited-state geometries with the B3-LYP[50] functional and TZVP[60] basis set. The anion geometries have been obtained from unrestricted B3-LYP calculations.

Excitation energies have been calculated using augmented triple-ζ valence basis set with polarization functions (the aug-cc-pVTZ basis set[61,62] for all atoms with one *f* function removed from each C atom and both *d* functions removed from each H atom) and the XCU1T[63] basis set for the LHF functional. These two basis sets are similar and almost equivalent in the number and diffuseness of basis functions.

For the CC2 calculations, a frozen space has been chosen which includes all core molecular orbitals (MOs) and all virtual MOs with an orbital energy greater than 120 eV. As an auxiliary basis set, we have used the aug-cc-pVTZ basis set[64] for all atoms with one *g* function removed from each C atom and both *f* functions removed from each H atom.

The basis set employed in these calculations has been chosen in order to give converged results in CC2 calculations. In fact DFT is known[65] to require smaller basis sets for a good description of conjugated systems than those required by correlated methods: in our tests on excited states of 3*T* already a TZVP basis set gives excitation energies not more than 0.01 eV different from those obtained with the aug-cc-pVTZ/XCU1T basis set. The choice of the basis set for the CC2 method instead needs more attention. In Figure 1, we report the differences between the excitation energies of the first singlet and of the two lowest triplet states of 3*T* computed with SV(P),[66] TZVP,[60] cc-pVTZ[67,68] and ATZVP[60] basis set, respectively, and the same excitation energies obtained employing the aug-cc-pVTZ basis set. The singlet state results are more sensitive to basis set dimensions and the excitation energies change by 0.36 eV going from SV(P) to aug-cc-pVTZ. The two triplet energies behave similarly to each other and are less basis set dependent, changing by about 0.15 eV going from SV(P) to aug-cc-pVTZ. Nevertheless, some general trends can be deduced: the inclusion of polarization functions highly improves the results, especially for triplets (42−53% of the total difference can be attributed to this effect); the inclusion of augmented functions highly improves the results, especially for the singlet (40−50% of the

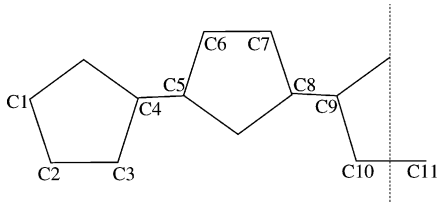

Figure 2. Numbering of atoms in 5*T*.

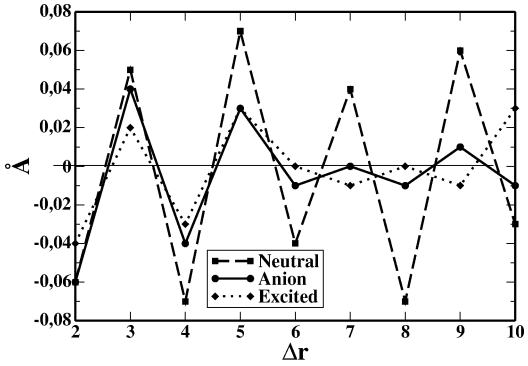

Figure 3. C-C bond length alternation (see text for details) in Å for different sites in 5*T*.

total difference can be attributed to this effect); the use of coupled cluster optimized basis functions moderately improves the results (27% of the total difference can be attributed to this effect).

All calculations have been performed with the TURBOMOLE[69] program package. In particular, the modules DSCF,[70] ESCF,[71] and the RICC2[56] have been used.

IV. Results

A. Geometries. An important quantity to analyze is the bond length alternation defined as $\Delta r_i \equiv |\vec{C}_i - \vec{C}_{i-1}| - |\vec{C}_i - \vec{C}_{i+1}|$, where $\vec{C}_i$ indicates the ith carbon atom position as in Figure 2. For 5*T* the bond length alternation for different sites is reported in Figure 3: the absence of aromatic character in the anion geometry and the appearance of a quinoid character in the S_1 geometry can be readily noticed.

In the neutral ground-state geometrical configuration, the oligomers present aromatic character. The inner rings of 3*T*, 4*T*, and 5*T* have the same geometric structure. The geometry of the terminal rings are different from that of the inner ones, resembling the structural properties of 2*T*. The inner part of the ring is equal to the internal rings and the outer part has Δr and a C−S bond length of 0.06 and 1.73 Å, respectively. These results are in agreement with previous MP2 calculations and X-ray data.[72]

In the anion ground-state geometrical configuration, in contrast with the former case, a regular behavior of the geometric structure of the inner rings is absent. In the longer oligomers, the central rings show an absence of bond length alternation and in general there is a shortening of bond length alternation Δr going from the outer to the inner part of the molecule. This can be ascribed to the occupation of LUMO that is bonding in nature with respect to the C−C inter-ring single bond and antibonding with respect the C−C double bonds and so tends to compress single bonds. The reliability of the computed anion geometry has been checked by optimizing 4*T* with the ATZVP[60] basis set. No meaningful differences can be noticed between the two optimized structures, and in particular, the same bond length alternation is predicted.

TABLE 1: Excitation Energies in eV Calculated with Different Methods for the Lowest Singlet Excited State Geometry[a]

state	transition	LDA	B−P	LHF	B3L	CC2	exp.
2T							
^1B_u	$4b_g \rightarrow 5a_u$	3.20	3.19	3.25	3.25	3.65	3.42
^3B_u	$4b_g \rightarrow 5a_u$	1.98	1.79	1.76	1.63	2.25	
^3A_g	$4b_g \rightarrow 7b_g$	3.58	3.42	3.39	3.39	3.89	
	$3a_u \rightarrow 5a_u$						
3T							
$^1B_1$	$5a_2 \rightarrow 8b_2$	2.60	2.60	2.65	2.69	3.10	2.90
$^3B_1$	$5a_2 \rightarrow 8b_2$	1.57	1.43	1.41	1.29	1.90	
$^3A_1$	$7b_2 \rightarrow 8b_2$	2.74	2.60	2.60	2.58	3.11	
	$5a_2 \rightarrow 6a_2$						
4T							
^1B_u	$8b_g \rightarrow 9a_u$	2.24	2.24	2.29	2.36	2.77	2.59
^3B_u	$8b_g \rightarrow 9a_u$	1.36	1.24	1.23	1.12	1.73	
^3A_g	$8b_g \rightarrow 9b_g$	2.24	2.13	2.12	2.10	2.63	
	$8a_u \rightarrow 9a_u$						
5T							
$^1B_1$	$9a_2 \rightarrow 12b_2$	1.99	1.99	2.04	2.14	2.56	2.41
$^3B_1$	$9a_2 \rightarrow 12b_2$	1.23	1.13	1.12	1.03	1.63	
$^3A_1$	$9a_2 \rightarrow 10a_2$	1.93	1.83	1.83	1.80	2.33	
	$11b_2 \rightarrow 12b_2$						

[a] B3L stands for B3-LYP. Experimental data are taken from ref 44.

TABLE 2: Excitation Energies in eV Calculated with Different Methods for the Anion Geometry[a]

state	transition	LDA	B−P	LHF	B3L	CC2	exp.
2T							
^1B_u	$4b_g \rightarrow 5a_u$	3.39	3.38	3.45	3.47	3.88	3.88
^3B_u	$4b_g \rightarrow 5a_u$	2.18	1.99	1.97	1.87	2.49	2.28
^3A_g	$4b_g \rightarrow 7b_g$	3.51	3.45	3.51	3.52	4.04	3.88[b]
	$3a_u \rightarrow 5a_u$						
3T							
$^1B_1$	$5a_2 \rightarrow 8b_2$	2.71	2.70	2.76	2.82	3.24	3.05
$^3B_1$	$5a_2 \rightarrow 8b_2$	1.71	1.56	1.55	1.45	2.06	1.92
$^3A_1$	$7b_2 \rightarrow 8b_2$	2.84	2.69	2.69	2.67	3.20	3.4
	$5a_2 \rightarrow 6a_2$						
4T							
^1B_u	$8b_g \rightarrow 9a_u$	2.31	2.31	2.36	2.46	2.88	2.69
^3B_u	$8b_g \rightarrow 9a_u$	1.46	1.34	1.33	1.24	1.85	1.76
^3A_g	$8b_g \rightarrow 9b_g$	2.32	2.20	2.20	2.17	2.71	3.13
	$8a_u \rightarrow 9a_u$						
5T							
$^1B_1$	$9a_2 \rightarrow 12b_2$	2.05	2.06	2.10	2.22	2.66	
$^3B_1$	$9a_2 \rightarrow 12b_2$	1.31	1.21	1.20	1.13	1.74	
$^3A_1$	$9a_2 \rightarrow 10a_2$	1.99	1.89	1.89	1.86	2.40	
	$11b_2 \rightarrow 12b_2$						

[a] B3L stands for B3-LYP. [b] Interpolated. See ref 7.

In the S_1 configuration, small distortions occur; it appears as a reduction in bond length alternation and the increase of a quinoid character on the inner thiophene rings. Similar results have been predicted at the MNDO[5] and CASSCF level.[9] Also in this case the effect can be interpreted in terms of the antibonding and bonding character of the highest occupied molecular orbital (HOMO) and lowest unoccupied molecular orbital (LUMO), respectively. In fact, according to TD-DFT and CC2 calculations (see later on) the S_1 state is essentially described by a HOMO → LUMO transition and this leads to slightly shorter single bonds and longer double bonds.

B. Excitation Energies. Excitations energies for the oligomers of thiophene *nT* with $n = 2-5$ for the three geometrical configurations are reported in Tables 1−3. As can be seen in these tables, various electronic and optical properties are common to all methods and geometries.

The lowest singlet and triplet excited states are almost completely described by a HOMO → LUMO transition, for all oligothiophenes. On the other hand, the second triplet state is

TABLE 3: Excitation Energies in eV Calculated with Different Methods for the Neutral Ground-State Geometry[a]

state	transition	LDA	B−P	LHF	B3L	CC2	exp.
2T							
^1B_u	$4b_g \rightarrow 5a_u$	3.68	3.68	3.75	3.83	4.26	4.05, 4.13[b]
^3B_u	$4b_g \rightarrow 5a_u$	2.59	2.41	2.40	2.36	2.95	
^3A_g	$4b_g \rightarrow 7b_g$	3.75	3.70	3.72	3.73	4.23	
	$3a_u \rightarrow 5a_u$						
3T							
$^1B_1$	$5a_2 \rightarrow 8b_2$	2.93	2.93	2.99	3.12	3.57	3.49
$^3B_1$	$5a_2 \rightarrow 8b_2$	2.04	1.90	1.90	1.87	2.46	
$^3A_1$	$7b_2 \rightarrow 8b_2$	3.03	2.88	2.88	2.88	3.42	
	$5a_2 \rightarrow 6a_2$						
4T							
^1B_u	$8b_g \rightarrow 9a_u$	2.51	2.50	2.57	2.73	3.21	3.16
^3B_u	$8b_g \rightarrow 9a_u$	1.76	1.65	1.65	1.64	2.23	
^3A_g	$8b_g \rightarrow 9b_g$	2.50	2.38	2.38	2.38	2.93	
	$8a_u \rightarrow 9a_u$						
5T							
$^1B_1$	$9a_2 \rightarrow 12b_2$	2.21	2.21	2.27	2.47	2.96	2.99
$^3B_1$	$9a_2 \rightarrow 12b_2$	1.58	1.48	1.49	1.49	2.08	
$^3A_1$	$9a_2 \rightarrow 10a_2$	2.16	2.05	2.06	2.06	2.61	
	$11b_2 \rightarrow 12b_2$						

[a] B3L stands for B3-LYP. Experimental data are taken from ref 75. [b] From ref 76.

more correlated and is mainly described by a mixing of HOMO-1 → LUMO (for bithiophene HOMO-3($3a_u$) → LUMO) and HOMO → LUMO+1 (in CC2 calculations HOMO → LUMO+N, with N>1) transitions. These transitions mix because they have very close single particle gaps. The percentage of these configurations (not reported for simplicity) depends on the method used (HOMO → LUMO+1 is always the largest). These molecular orbitals all have π character. As an example, the orbitals from the B3-LYP calculation are reported in Figure 4 for quarter-thiophene.

In Figure 5, the B3-LYP molecular orbital energies and single particle gaps for the excited-state geometry are reported as function of $1/n$, as it is usually done for oligomers. Other methods/geometries show similar trends for orbital energies vs $1/n$, whereas, as it will be discussed later on, the absolute values of the energy gaps are different. Figure 5 shows that with increasing chain length the HOMO-1 → LUMO and HOMO → LUMO+1 energy gaps become closer. Mixing of these configurations is therefore facilitated. Figure 5 also displays the different chain length dependence of various orbitals and transition energies. The HOMO-1 (LUMO+1) has a faster increase (decrease) of the energy as compared to the HOMO (LUMO). Indeed the HOMO-1 (LUMO+1) has one more nodal plane than the HOMO (LUMO), i.e., (see Figure 4) the phase of the orbital of the two monomers on the right changes going from HOMO(LUMO) to HOMO-1(LUMO+1). Thus, the HOMO-1 → LUMO and the HOMO → LUMO+1 energy gaps decrease faster with the chain length than the HOMO → LUMO ones.

The KS energy-gaps are important quantities because they represent a zero-order approximation to TD-DFT excitation energies.[73] It turned out that energy-gaps (and see later on, excitation energies) for all TD-DFT methods and geometries can be fitted with the expression of the extended free electron model (FEMO):[7,74]

$$E_n = \frac{\alpha}{4n+1} + \beta\left(1 - \frac{1}{4n}\right) \quad (1)$$

with a very small deviation (i.e., an rms value of only 0.018 eV, averaged over all TD-DFT gaps/methods/geometries). The FEMO model takes into account (through the β coefficient) the finite energy-gap for $n \rightarrow +\infty$. The α value describes the relative decrease of energy-gaps with increasing chain length. The α value can be used to quantitatively estimate the differences between DFT methods. We note that eq 1 shows a small nonlinear behavior when it is plotted against $1/n$. Calculated energy gaps (and see later on excitation energies) also show this small nonlinearity when they are plotted vs $1/n$, so that eq 1 is, for small n, superior to a simple linear expression, i.e., $E_n = \beta + \alpha/n$. The α values of the HOMO → LUMO,

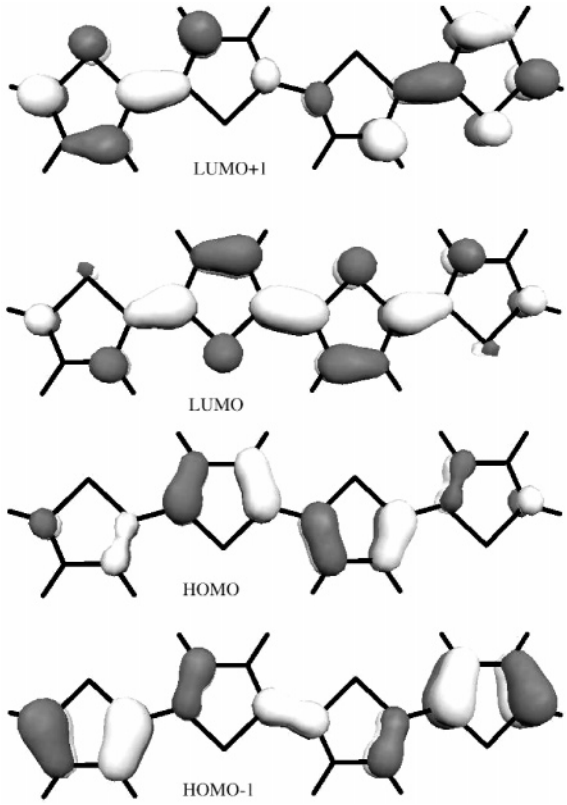

Figure 4. HOMO-1, HOMO, LUMO, and LUMO+1 wave function as obtained by a B3-LYP calculation in the excited-state geometry for 4*T*.

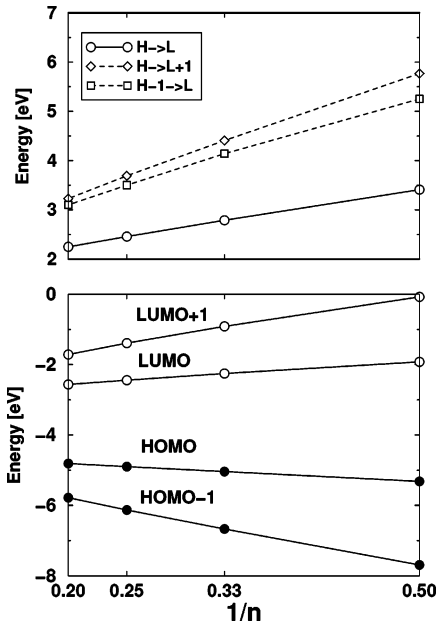

Figure 5. Molecular orbital energies (lower panel) and single-particle transitions, i.e., KS eigenvalues gap, (upper panel) from B3-LYP calculations for excited-state geometries.

TABLE 4: α Values (See Text for Definition) for Single-Particle Transitions in eV*Monomer for Different Methods[a]

transition	LDA	B−P	LHF	B3L
excited				
HOMO → LUMO	15.0	15.2	15.7	19.9
HOMO-1 → LUMO	35.4	35.3	36.0	41.5
HOMO → LUMO+1	29.7	30.0	30.3	35.6
anion				
HOMO → LUMO	17.2	17.2	17.7	22.0
HOMO-1 → LUMO	35.9	35.8	36.3	42.0
HOMO → LUMO+1	31.7	32.1	32.5	37.9
neutral				
HOMO → LUMO	19.2	19.4	20.0	23.9
HOMO-1 → LUMO	36.7	36.6	37.3	42.7
HOMO → LUMO+1	32.1	32.4	32.8	38.0

[a] B3L stands for B3-LYP.

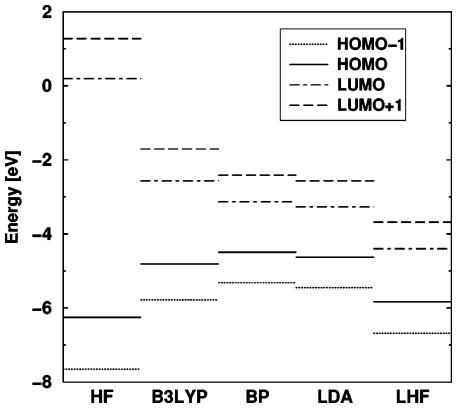

Figure 6. Energies of molecular orbitals for various methods for 5*T* in the excited-state geometry.

HOMO-1 → LUMO, HOMO → LUMO+1 energy-gaps are summarized in Table 4. The β-values are not relevant for this work because they mainly represent the energy gap of the polymer and have a negligible effect on chain-length dependence (note that $\beta \ll \alpha$ so that the second term in eq 1 has a negligible dependence with n). Later on, the β values for photoluminescence will be given. For all methods and geometries, the α values for HOMO-1 → LUMO and HOMO → LUMO+1 energy-gaps are larger than the ones for HOMO → LUMO. Table 4 also shows that all energy-gaps increase with the nonlocality of the exchange functional, i.e., (from left to right in the tables) in the order LDA (local Slater-Dirac), B−P (gradient-corrected), LHF (orbital-dependent), and B3-LYP (which contains 20% of the nonlocal HF exchange). The increase of the inter-ring C−C bond length of the molecular geometry (i.e., in the order excited, anion, and neutral ground-state geometry) causes an increase of the energy-gaps.

Although the chain length dependence of orbital energies is quite similar for the different methods, their absolute values are strongly different as shown in Figure 6. Largest differences are present for unoccupied orbitals which are unbound (i.e., exhibit positive energies) in HF and bound (i.e., with negative energies) in DFT methods. In LHF, unoccupied orbitals are even more bound, because LHF is a self-interaction free method[54] and the resulting potential is more attractive. Occupied orbitals with conventional XC functionals are higher in energy than those from HF and LHF. The latter two yield very close occupied orbital eigenvalues because in the LHF method the exchange potential is de facto an exact local exchange potential.[54] Despite large differences in the absolute energies, all pure (i.e., non-hybrid) KS energy gaps are quite close each other. In the hybrid B3-LYP, the orbitals energies, on the other hand, lie between HF and KS methods, due to the presence of the nonlocal HF exchange in the B3-LYP potential.

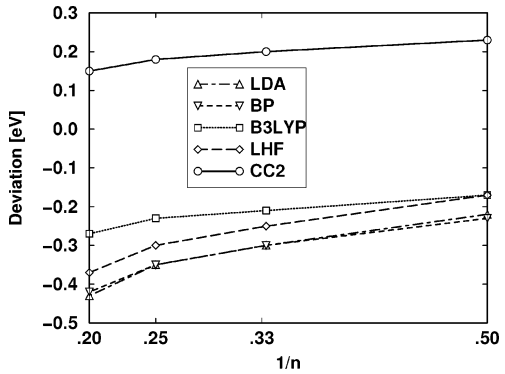

Figure 7. Difference between theoretical and experimental photoluminescence energies vs the inverse of the number of monomers for different methods.

Excitation energies in Tables 1 and 2 can be compared to photoluminescence[44] and PD-PES[7] measurements, respectively. Absorption energies[75] are reported in Table 3, but we point out that an exact comparison of neutral ground-state excitation energies with experimental data is not possible due to the employed planar geometries. The mean absolute error (MAE) for those excitations for which experimental results are available, are reported in Table 3. For the ^{1}B state, the CC2 method is the best in reproducing absolute emission energies and PD-PES. B−P gives results close to LDA, whereas the use of self-interaction free LHF orbitals and eigenvalues improves the agreement with experiments. The use of a hybrid functional gives results closer to CC2.

For the lowest triplet ^{3}B state, the situation is different. The use of a more accurate exchange functional reduces the agreement with experimental results, whereas LDA gives results close to CC2. This apparently surprising result will be discussed later on. For the second triplet, problems are clearly present in all methods. All TD-DFT methods as well as CC2 deviate by about half an eV from the experimental value.

The evolution of the excitation energies with the chain length also follows the relation (1), again with a very small deviation (the average rms value is 0.046 eV). In Figure 7, we report photoluminescence emission energy (i.e., excitation energy for the S_1 state in the S_1 geometry) deviations from experiments for different methods. Figure 7 shows that CC2 results overestimate the experimental photoluminescence data whereas all TD-DFT methods underestimate them. In TD-DFT, the deviation from experiments *increases* with the chain length. This is a behavior also found for other conjugated chainlike systems[26−29] and is related to the approximations in the XC kernel. However, at least for the relatively small number of monomers considered in this work, the deviations from experiments are quite small. For example, going from $n = 2$ to 5, the TD-LDA deviation from experiment increases by only 0.2 eV, which is below the absolute accuracy. Figure 7 shows that all methods (in particularly B3-LYP and CC2) have a similar $1/n$ behavior; that is, all of the curves in Figure 7 look quite similar and are only shifted vertically. Thus, these methods have quite similar α values and different values of β. This is quantitatively confirmed by Table 6, where the α values for all excited states and geometries are reported. Note that the α values are very sensible quantities. For example, Table 6 shows that the CC2 α value for photoluminescence is 19.2 eV*monomer whereas the experimental value is 17.8 eV*monomer, which means a

TABLE 5: Mean Absolute Errors of Excitation Energies in EV for Different Methods in Comparison with Experimental Data. B3L Stands for B3-LYP

geom.	state	LDA	B−P	LHF	B3L	CC2
excited	^{1}B	0.32	0.33	0.27	0.22	0.19
anion	^{1}B	0.40	0.41	0.30	0.29	0.13
anion	^{3}B	0.20	0.36	0.47	0.47	0.15
anion	^{3}A	0.50	0.57	0.61	0.61	0.43

TABLE 6: α Values (See Text for Definition) for Excitation Energies in eV*Monomer for Different Methods[a]

state	LDA	B−P	LHF	B3L	CC2	exp.
excited						
^{1}B	20.2	20.1	20.3	18.9	19.2	17.8
^{3}B	12.6	11.2	10.8	10.2	11.2	
^{3}A	26.8	25.7	25.3	25.7	25.9	
anion						
^{1}B	22.3	22.0	22.5	21.1	21.3	24.5[b]
^{3}B	14.5	13.0	12.9	12.4	13.3	11.4[b]
^{3}A	26.0	25.3	26.3	26.8	27.2	17.0[b]
neutral						
^{1}B	24.3	24.4	24.7	23.0	22.7	
^{3}B	16.9	15.5	15.3	14.7	15.4	
^{3}A	26.1	26.8	27.0	27.2	27.1	

[a] B3L stands for B3-LYP. [b] Fit on 2*T*, 3*T*, and 4*T*.

deviation of about 10%. However, this deviation has little effect because it means that going from $n = 2$ to 5 the difference in absolute energies is less than 0.1 eV.

For the ^{1}B state (in excited-state geometry), all of the methods overestimate the experimental value. Compared to CC2, B3-LYP gives the closest α value, whereas other DFT methods overestimate them in all geometries, as can also be seen in Figure 7. B3-LYP has an α value (18.9 eV*monomer) smaller than CC2 (19.2 eV*monomer) which would mean even a better agreement with experiments; however, as discussed above, such small deviations are not significant.

The evolution of singlet excitation energies going from the excited-state geometry toward the neutral ground-state one, i.e., going from a quinoid to aromatic character, shows an increase of the α values for all of the states, both singlet and triplets. This is directly related to the α values of the energy gaps of Table 4: the more quinoid the geometry, the lower the α value. For the anion geometry, CC2 underestimates the PD-PES slopes, so that DFT methods are in slightly better agreement with the experiment. The corresponding β values for the singlet states ^{1}B in the excited state geometries are 1.10, 1.12, 1.16, 1.32, and 1.75 eV respectively, for the employed methods. These values clearly show the nonvanishing energy-gap for the polythiophene and they can, in principle, be compared with the luminescence energy of polythiophene, i.e., about 1.6 eV.[77]

Looking to the α values of ^{3}B state, we find that all methods give comparable values, with the exception of the LDA ones which have the largest values. In the anion geometry, LDA exhibits the largest deviation from experimental value. This is opposite to what we found in discussing the MAE, where it was found that the LDA gives the best triplet excitation energies. It turned out that the MAE of LDA is the smallest because the absolute values of excitation energies are higher (see Tables 1, 2 and 3), but the LDA chain dependence is less accurate than that of other XC functionals. Concerning the dependence on geometries, it is found again that the α values increase with less quinoid geometries.

For the ^{3}A state, the situation strongly changes. The α values are much higher, and no trend with the geometry can be recognized. The quinoid (anion) conformation is the most (least) sensitive to the length of the oligomer. As already pointed out in describing the MAE, the agreement with experiments is lost. The PD-PES experimental slope is about 17 eV*monomer which is completely different from the calculated values in the range 25−27 eV*monomer for all methods. This shows that there is a clear discrepancy between theory and experiment for the second triplet excitation energy.

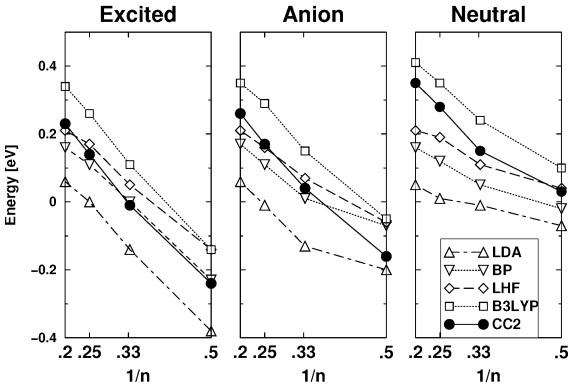

Figure 8. ^{1}B − ^{3}A energy difference versus the inverse of the number of monomers in the neutral and anionic ground state and *S*1 excited-state geometries.

V. Discussion

In Figure 8, we report the ^{1}B − ^{3}A energy difference as a function of $1/n$ for the various geometries and methods.

We note that there is a significant shift of ^{1}B − ^{3}A energy differences using different methods. For example, in the terthiophene excited geometry, LDA predicts the ^{3}A state above the ^{1}B state,[8] whereas the situation is reversed in other methods. For longer oligomers, the energy of the ^{3}A state goes below that of the ^{1}B state for all methods, but a spread of values as large as 0.3 eV is present. Note that these deviations are not systematic errors, because they are related to the differences of two excitation energies.

The ^{1}B − ^{3}A energy difference is also very sensible to the geometry. For bithiophene B3-LYP predicts the ^{1}B state energetically above the ^{3}A state for the neutral ground-state geometry but the situation is opposite for the excited-state geometries. This is an important point in discussing photophysical properties. The ^{1}B − ^{3}A energy difference increases going from the neutral ground state to the excited-state geometry. The chain-length dependence of the ^{1}B − ^{3}A energy difference is thus enhanced with decreasing inter-ring C−C bond length.

Even if different methods and geometries give different ^{1}B − ^{3}A values, Figure 8 clearly shows that the ^{1}B − ^{3}A energy difference is increasing with the number of rings for all geometries and for all methods. Thus for longer oligomers, we can definitely expect that the ^{3}A state will lie energetically below the ^{1}B state. This can also be inferred from the α values reported in Table 6 where the calculated α values of the ^{3}A state are always larger than the ones of the ^{1}B state. This effect can be traced back to the single particle transitions reported in Table 4. As already pointed out, the HOMO-1 → LUMO and HOMO → LUMO+1 α values are much larger than HOMO → LUMO. TD-DFT coupling contributions (i.e., the difference between the excitation energy and the single-particle eigenvalue difference of the dominant single particle transition) increase the α values for singlet transitions and decrease them for triplet ones. For example, the difference between the ^{1}B state and the ^{3}A state α values for LDA in the excited-state geometry is −6.6

eV*monomer, whereas in a single-particle approximation, it is −14.7 eV*monomer. Thus, TD-DFT coupling contribution reduces the α-value difference between the ^{1}B state and the ^{3}A state, but less than 50%.

This result is in complete disagreement with the findings of ref 7, where a positive α value (7.5 eV*monomer) was predicted. Our results obtained with first-principles methods and applied to different geometries lead to a negative slope for the α values difference between the ^{1}B state and the ^{3}A state in the anion geometry, in the range of 3.3−5.9 eV*monomer.

Possible shortcomings of our methods might be related to the ionic character of the A state.[78] TD-DFT is known to incorrectly describe charge-transfer effects.[28,79] We have checked whether this issue is relevant here by considering the TD-DFT excitation energies behavior with an increasing amount of HF exchange. We have computed the excitations of 4*T* with PBE0[47] and BH-LYP[80] functionals which have 25% and 50%, respectively, of Hartree−Fock exchange. Although the PBE0 results are almost identical to the B3-LYP ones, BH-LYP roughly shifts down all of the excited state by about (0.3 eV), but the same ordering of the states is preserved. Thus, we can conclude that the ionic character of these excited states, at least for the relative small number of monomers considered in this work, is of minor importance. The general trend that we observe (i.e., two triplet states below the singlet state for longer oligomers) is thus a real property of the system under examination.

The CC2 results may be thought to be incorrect because of the approximate treatment of the double excitations and the neglection of higher excitations. However, the computed states all have a large single excitation contribution (for singlet 91.6−92.8%; for triplet 97.5−98.3%, for the anion conformation), and the excitation energies can therefore be considered well converged with respect to the inclusion of higher order substitutions. This means that computed excitation energies are corrected through second order.[57,58] Also CC2 calculations performed on similar π systems yielded good results.[28,56] Moreover CC2 has been observed to slightly underestimate singlet energies[45] and to overestimate triplet energies:[57] this observation strengthens our conclusion that the ^{3}A state is below the ^{1}B state.

Thus, we believe that more accurate approaches cannot reverse these findings. Moreover, increasing the accuracy of the methods, i.e., going from LDA to CC2, increases the absolute value of the α-value difference between the ^{1}B state and the ^{3}A state. Our finding is also in agreement with the recent CASPT2 calculation on bithiophene,[9] where the PD-PES assignment of Rentsch et al. was refused.

Because of the inconsistency of the previous assignment of experiments reported in ref 7 with the theoretical results presented here, we conclude that some high lying triplets were detected instead of the second one.

We thus have calculated the 2^3B and the 2^3A excitation energies in the anion conformation with all of the previous methods. In Figure 9, we report the energies of the third PD-PES peak (which in ref 7 were assigned to the second triplet state) and compare them with the energies of the 2^3B state as computed by the different methods in the anion conformation. This comparison is motivated by the fact that due to symmetry considerations the B states should have larger amplitudes in PD-PES spectra, whereas the lower amplitudes of the A states might be undetected due to close proximity to other states. Figure 9 shows that very good agreement with experiment is found for all of the TD-DFT methods, confirming the 2^3B assignment. CC2 overestimates the PD-PES results, nevertheless it predicts correctly the general trend.

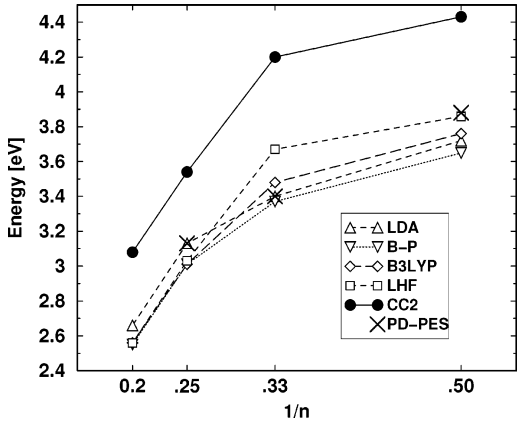

Figure 9. Energies of the third PD-PES peak and of the 2^3B state as computed by LDA, B−P, B3-LYP, LHF, and CC2 methods, in the anion conformation.

Note that the 2^3B state is the actually the fourth triplet state, except in 3*T* and 4*T* with the CC2 and the B3-LYP approach where it is the third: these two methods thus present a symmetry-crossing with chain-length evolution between the 2^3B state and the 2^3A state. This is also in agreement with the CASPT2 calculations on bithiophene,[9] where two triplets were found below the 2^3B state. For these high lying triplets, a linear trend vs 1/*n* is absent because the contributing configuration strongly change with the chain length. Note that these lowest triplet states of A symmetry cannot be well investigated by triplet−triplet absorption measurements because the latter is dominated by a peak involving only higher triplet A states.[5,9,44]

We conclude that the second PD-PES peak which has been assigned to S_1 actually contains both the S_1 and T_2 (1^3A) states which are predicted to be quite close to each other. The third PD-PES peak cannot be assigned to T_2, instead it has to be assigned to the third (or the forth) triplet state 2^3B.

VI. Conclusions

We have studied the evolution of the singlet and triplet excitation energies in oligothiophenes as a function of the chain length. We have compared different first-principles TD-DFT methods with CC2 results and experiments. We found that the CC2 results exhibit the best absolute agreement with experimental emission energies. TD-DFT methods underestimate experimental excitation energies. This underestimation increases with the chain length as already found in other chain like systems. However, for the number of monomers considered here, the chain-length evolution (i.e., α values) is still quite reliable, especially with an hybrid DFT kernel. An absolute determination of the $S_1 - T_2$ gap is difficult, because it strongly depends on the method and geometry. However, all methods show that the second triplet state lies energetically below the first singlet excited state for long oligomers. This finding shows that the PD-PES assignment of Rentsch et al. needs to be reconsidered. The third experimental peak that was previously assigned to the second triplet state must be instead assigned to the 2^3B state, which is energetically the third or the fourth one. We believe that the results presented in this work will be of fundamental importance for the future photophysical investigations of oligothiophenes.

Acknowledgment. We thank R. Ahlrichs for providing the TURBOMOLE program package, C. Hättig for technical discussions, and G. Aloisio for his support. The calculations were carried out at the CACT/ISUFI (Lecce).

References and Notes

(1) *Handbook of Organic Conductive Molecules and Polymers*; Nalwa, H. S.; J. Wiley & Sons: Chichester, U.K., 1997.

(2) Friend, R. H. et al. *Nature* **1999**, 397, 121.

(3) Müllen, K.; Wegner, G. *Electronic Materials: The Oligomer Approach*; Wiley-VCH: New York, 1998.

(4) Taliani, C.; Gebauer, W. *Handbook of Oligo and Polythiophenes*; Fichou, D., Ed.; Wiley-VCN: Weinheim, Germany, 1999.

(5) Beljonne, D.; Cornil, J.; Friend, R. H.; Janssen, R. A. J.; Brèdas, J. L. *J. Am. Chem. Soc.* **1996**, *118*, 6453.

(6) Yang, J. P.; Paa, W.; Rentsch, S. *Chem. Phys. Lett.* **2000**, *320*, 665.

(7) Rentsch, S.; Yang, J. P.; Paa, W.; Birckner, E.; Schiedt, J.; Weinkauf, R. *Phys. Chem. Chem. Phys.* **1999**, *1*, 1707.

(8) Della Sala, F.; Heinze, H. H.; Görling, A. *Chem. Phys. Lett.* **2001**, *339*, 343.

(9) Rubio, M.; Merchán, M.; Pou-Amérigo, R.; Ortí, E. *Chem. Phys. Chem.* **2003**, *4*, 1308.

(10) De Oliveira, M. A.; Duarte, H. A.; Pernaut, J.; De Almeida, W. B. *J. Phys. Chem. A* **2000**, *104*, 8256.

(11) Brèdas, J. L. *J. Chem. Phys.* **1985**, *82*, 3808.

(12) Belletête, M.; DiCesare, N.; Leclerc, M.; Durocher, G. *Chem. Phys. Lett.* **1996**, *250*, 31.

(13) Colditz, R.; Grebner, D.; Helbig, M.; Rentsch S. *Chem. Phys.* **1995**, *201*, 309.

(14) Cornil, J.; Belijonne, D.; Brédas, J. L. *J. Chem. Phys.* **1995**, *103*, 842.

(15) Belijonne, D.; Shuai, Z.; Brédas, J. L. *J. Chem. Phys.* **1993**, *98*, 8819.

(16) Tozer, D. J.; Amos, R. D.; Handy, N. C.; Roos, B. O.; Serrano-Andrés, L. *Mol. Phys.* **1999**, *97*, 859.

(17) Serrano-Andrés, L.; Merchán, M.; Fülscher, M.; Roos, B. *Chem. Phys. Lett.* **1993**, *211*, 125.

(18) Wan, J.; Hada, M.; Ehara, M.; Nakatsuji, H. *J. Chem. Phys.* **2001**, *114*, 842.

(19) Rubio, M.; Merchán, M.; Orti, E.; Roos, B. O. *J. Chem. Phys.* **1995**, *102*, 9.

(20) Gross, E. K. U.; Kohn, W. *Phys. Rev. Lett.* **1985**, *85*, 2850.

(21) van Gisbergen, S. J. A.; Snijders, J. G. and Baerends, E. J. *J. Chem. Phys.* **1995**, *103*, 9347.

(22) Jamorski, C.; Casida, M. E.; Salahub, D. R. *J. Chem. Phys.* **1996**, *104*, 5134.

(23) Casida, M. E. Recent Developments and Applications of Modern Density Functional Theory. In *Theoretical and Computational Chemistry Vol. 4*; Seminario, J. M., Ed.; Elsevier Science: Amsterdam, 1996; p 391.

(24) Gross, E. K. U.; Dobson, J. F.; Petersilka, M. Density Functional Theory II. In *Vol. 181 of Topics in Current Chemistry*; Nalewajski, R. F., Ed.; Springer: Berlin, 1996; p 81.

(25) Bauernschmitt, R.; Ahlrichs, R. *Chem. Phys. Lett.* **1996**, *256*, 454.

(26) Cai, Z. L.; Sendt, K.; Reimers, J. R. *J. Chem. Phys.* **2002**, *117*, 5543.

(27) Hsu, C. P.; Hirata, S.; Head-Gordon, M. *J. Phys. Chem. A* **2001**, *105*, 451.

(28) Grimme, S.; Parac, M. *Chem. Phys. Chem.* **2003**, *4*, 292.

(29) Weimer, M.; Hieringer, W.; Della Sala, F.; Görling, A. *Chem. Phys.* **2005**, *309*, 77.

(30) Houck, K. N.; Lee, P. S.; Nendel M. *J. Org. Chem.* **2001**, *66*, 5517.

(31) van Gisbergen, S. J. A.; Schipper, P. R. T.; Gritsenko, O. V.; Baerends, E. J.; Snijders, J. G.; Champagne, B.; Kirtman, B. *Phys. Rev. Lett.* **1999**, *83*, 694.

(32) Yu, J.-S. K.; Chen, W.-C.; Yu, C.-H. *J. Phys. Chem A* **2003**, *107*, 4268.

(33) Han, Y.-K.; Lee, S. U. *J. Chem. Phys.* **2004**, *121*, 609.

(34) Han, Y.-K. *J. Phys. Chem. A* **2004**, *108*, 9316.

(35) Zhu, Z.; Wang, Y.; Lu, Y. *Macromolecules* **2003**, *36*, 9585.

(36) Wang, J.; Feng, J.; Ren, A.; Liu, X.; Ma, Y.; Lu, P.; Zang, H. *Macromolecules* **2004**, *37*, 3451.

(37) Telesca, R.; Bolink, H.; Yunoki, S.; Hadziioannou, G.; Van Duijnen, P. Th.; Snijders, J. G.; Jonkman, H. T.; Sawatzky, G. A. *Phys. Rev. B* **2001**, *63*, 155112.

(38) Pogantsch, A.; Heimel, H.; Zojer, E. *J. Chem. Phys.* **2002**, *117*, 5921.

(39) Hutchinson, G. R.; Ratner, M. A.; Marks, T. J. *J. Phys. Chem. A* **2002**, *106*, 10596.

(40) Foresman, J. B.; Head-Gordon, M. People, J. A.; Frish, M. J. *J. Phys. Chem.* **1992**, *96*, 135.

(41) Furche, F.; Ahlrichs, R. *J. Chem. Phys.* **2002**, *117*, 7433.

(42) Della Sala, F.; Raganato, M. F.; Anni, M.; Cingolani, R.; Weimer, M.; Görling, A.; Favaretto, L.; Barbarella, G.; Gigli, G. *Synth. Met.* **2003**, *139*, 897.

(43) Raganato, M. F.; Vitale, V.; Della Sala, F.; Anni, M.; Cingolani, R.; Gigli, G.; Favaretto, L.; Barbarella, G.; Weimer, M.; Görling, A. *J. Chem. Phys.* **2004**, *121*, 3784.

(44) Becker, R. S.; de Melo, J. S.; Macanita, A. L.; Elisei, F. *J. Phys. Chem.* **1996**, *100*, 18683.

(45) Christiansen, O.; Koch, H.; Jørgensen, P. *Chem. Phys. Lett.* **1995**, *234*, 409.

(46) Shuai, Z.; Bredas, J. L. *Phys. Rev. B* **2000**, *62*, 15452.

(47) Perdew, J. P.; Burke, K.; Ernzerhof, M. *Phys. Rev. Lett.* **1996**, *77*, 3865.

(48) Becke, A. D. *Phys. Rev. A* **1988**, *38*, 3098.

(49) Perdew, J. P. *Phys. Rev. B* **1986**, *33*, 8822.

(50) Becke, A. D. *J. Chem. Phys.* **1993**, *98*, 5648.

(51) Parr, R. G.; Yang, W. *Density Functional Theory of Atoms and Molecules*; Oxford University Press: New York, 1989.

(52) Dreizler, R. M.; Gross, E. K. U. *Density Functional Theory*; Springer: Heidelberg, Germany, 1990.

(53) Koch, W.; Holthausen, M. *A Chemist's Guide to Density Functional Theory*; Wiley-VCH: New York, 2000.

(54) Della Sala, F.; Görling, A. *J. Chem. Phys.* **2001**, *115*, 5718.

(55) Della Sala, F.; Görling, A. *J. Chem. Phys.* **2002**, *116*, 5374.

(56) Hättig, C.; Weigend, F. *J. Chem. Phys.* **2000**, *113*, 5154.

(57) Larsen, H.; Hald, K.; Holsen, J.; Jørgensen, P. *J. Chem. Phys.* **2001**, *115*, 3015.

(58) Christiansen, O.; Koch, H.; Jørgensen, P. *J. Chem. Phys.* **1996**, *105*, 1451.

(59) Schiedt, J.; Weinkauf, R. *J. Chem. Phys.* **1999**, *110*, 304.

(60) Schäfer, A.; Huber, C.; Ahlrichs, R. *J. Chem. Phys.* **1994**, *100*, 5829.

(61) Dunning Jr, T. H. *J. Chem. Phys.* **1989**, *90*, 1007.

(62) Kendall, R. A.; Dunning Jr., T. H.; Harrison, R. J. *J. Chem. Phys.* **1992**, *96*, 6769.

(63) Della Sala, F.; Görling, A. *J. Chem. Phys.* **2003**, *118*, 10439.

(64) Weigend, F.; Köhn, A.; Hättig, C. *J. Chem. Phys.* **2002**, *116*, 3175.

(65) Bauschlinger, C. W.; Ricca, A.; Partridge, H.; Langhoff, S. R. Recent Advances in Density Functional Methods Part II. In *Chemistry by Density Functional Theory*; Chong, D. P., Ed.; World Scientific: Singapore, 1997.

(66) Shäfer, A.; Horn, H.; Ahlrichs, R. *J. Chem. Phys.* **1992**, *97*, 2571.

(67) Dunning Jr., T. H. *J. Chem. Phys.* **1989**, *90*, 1007.

(68) Woon, D. E.; Dunning, T. H., Jr. *J. Chem. Phys.* **1993**, *98*, 1358.

(69) Ahlrichs, R. et al., *TURBOMOLE*; University of Karlsruhe: Germany, 1988.

(70) Treutler, O.; Ahlrichs, R. *J. Chem. Phys.* **1995**, *102*, 346.

(71) Bauernschmitt, R.; Ahlrichs, R. *Chem. Phys. Lett.* **1996**, *256*, 454.

(72) Ortí, E.; Viruela, P. M.; Sánchez-Marín, J.; Tomás, F. *J. Phys. Chem.* **1995**, *99*, 4955.

(73) Görling, A. *Phys. Rev. A* **1996**, *54*, 3912.

(74) Grebner, D.; Helbig, M.; Rentsch, S. *J. Phys. Chem.* **1995**, *99*, 16991.

(75) Lap, D. V.; Grebner, D.; Rentsch, S. *J. Phys. Chem. A* **1997**, *101*, 107.

(76) Chadwick, J. E.; Kohler, B. E. *J. Phys. Chem.* **1994**, *98*, 3631.

(77) Sakurai, K.; Tachibana, H.; Shiga, N.; Terakura, C.; Matsumoto, M.; Tokura, Y. *Phys. Rev. B* **1997**, *56*, 9552.

(78) van der Horst, J. W.; Bobbert, P. A.; de Jong, P. H. L.; Michels, M. A.; Brocks, G.; Kelly, P. J. *Phys. Rev. B* **2000**, *61*, 15187.

(79) Dreuw, A.; Head-Gordon, M. *J. Am. Chem. Soc.* **2004**, *126*, 4007.

(80) Becke, A. D. *J. Chem. Phys.* **1993**, *98*, 1372.